Nat. Hazards Earth Syst. Sci. Discuss., https://doi.org/10.5194/nhess-2017-416
Manuscript under review for journal Nat. Hazards Earth Syst. Sci.
Discussion started: 5 December 2017

Natural Hazards and Earth System Sciences
Discussions

Temporal evolution of landslide hazard for a road infrastructure in the Municipality of Nocera Inferiore, Italy, under the effect of climate change

Marco Uzielli[1,2], Guido Rianna[3], Fabio Ciervo[3], Paola Mercogliano[3,4], Unni K. Eidsvig[2]

[1] Georisk Engineering S.r.l., Firenze, 50132, Italy
[2] NGI (Norwegian Geotechnical Institute), Oslo, 0855, Norway
[3] CMCC Foundation (Centro Euro-Mediterraneo sui Cambiamenti Climatici), Capua, 81043, Italy
[4] CIRA (Centro Italiano Ricerche Aerospaziali), Capua, 81043, Italy

Correspondence to: Marco Uzielli (muz@georisk.eu)

Abstract. In recent years, landslide events have extensively affected pyroclastic covers of the Campania Region in southern Italy, causing victims and conspicuous economic damages. Due to the high criticality of the area, a proper assessment of future variations in landslide occurrences and related risk is crucial for policy-makers, administrators and infrastructure stakeholders. This paper addresses work performed within the FP7 INTACT project, having the goal to provide a risk framework for critical infrastructure while accounting for climate change. The study is a part of the testing and application of the framework in the Campania region, assessing the temporal variation in landslide hazard specifically for a section of the Autostrada A3 "Salerno-Napoli" motorway, which runs across the toe of the Monte Albino relief in the Municipality of Nocera Inferiore. In the study, hazard is defined as the yearly probability of a spatial location within a study area to be affected by landslide runout given the occurrence of rainfall-related triggering conditions. Hence, hazard depends both on the likelihood of rainfall-induced landslide triggering within the study area and the likelihood that the specific location will be affected following landslide runout. Landslide triggering probability is calculated through the application of Bayesian theory and relying on local historical rainfall data. Temporal variations in triggering probability due to climate change are estimated from present-day to the year 2100 through the characterization of rainfall patterns and related uncertainties using the EURO-CORDEX Ensemble. Reach probability, defining the probability that a given spatial location is affected by debris flows, is calculated spatially through numerical simulation of landslide runout. The temporal evolution of hazard is investigated specifically in the proximity of the motorway, as to provide a quantitative support for landslide risk analysis.

1 Introduction

In recent years, eminent scholars have debated about the main features of “shallow” and “deep” uncertainties in assessment of natural hazards (Stein & Stein 2013; Hallegatte et al. 2012; Cox 2012). While probability distributions of "shallow" uncertainties in outcomes are “reasonably well known” (Stein & Stein 2012), "deep" uncertainties refer to: (1) several possible

future worlds without known relative probabilities; (2) multiple conflicting but equally-reasonable world-views (3) adaptation strategies with remarkable feedbacks among the sectors (Hallegatte et al. 2012).

As stressed in these works, the issue of climate change issue and its impacts can be considered “a fantastic example of 'very deep' uncertainty". Nevertheless, given the extent of potential impacts on communities (Paris Agreement 2015) including their economic dimension (Stern 2006; Nordhaus 2007; Chancel & Piketty 2015), considerable efforts have been spent in recent years devoted to assessing the variations in frequency and magnitude of weather-induced hazards related to climate changes (Seneviratne et al. 2012). A variety of strategies have been devised and implemented with the aim of detecting the main sources of uncertainty and their extent (Wilby & Dessai 2010; Cooke 2014; Koutsoyiannis & Montanari 2012; Beven 2015).

Among weather-induced hazards, investigations on future trends in the occurrence and consequences of landslides and on the uncertainties in their estimation have received relatively limited interest (Gariano & Guzzetti 2016; Beven et al. 2015). Possible concurrent causes include the mismatch between the usual scale of analysis for landslide case studies and the current horizontal resolutions of climate projections, as well as the extraordinarily relevant role of case-specific geomorphological features, which hinder the generalization of findings to other contexts.

1.1 Previous studies of pyroclastic landslides in Campania

Despite the above limitations and, indeed, in the attempt to address them, several recent studies have focused on future variations in the occurrence of landslides affecting pyroclastic covers mantling the carbonate bedrocks in the Campania Region in Southern Italy. These studies considered different test cases; namely: Cervinara (Damiano & Mercogliano 2013; Rianna et al. 2016), Nocera Inferiore (Reder et al. 2016; Rianna et al. 2017a, 2017b) and Ravello (Ciervo et al. 2016). Several aspects differentiate the case studies and, consequently, the investigations performed in them. For example, depth, stratigraphy and grain size of pyroclastic covers are fundamentally regulated by slope, distance to volcanic centres (Campi Flegrei and Somma-Vesuvio), as well as wind direction and magnitude during the eruptions; such differences induce variations in rainfall patterns recognized as effective for slope failure (e.g. intensity, length of antecedent precipitation time window). For these reasons, while daily weather forcing data have been found to result in better assessments for the Cervinara and Nocera Inferiore test cases, sub-daily data have been found to improve the quality of assessments for the Ravello test case. Consequently, daily observations modified according to projected anomalies (Damiano & Mercogliano 2013) or daily data provided by climate simulations subjected to statistical bias correction are used in the former cases, while a stochastic approach is adopted with bias-corrected data to provide assessments at hourly scale for the latter. Moreover, in some studies (Reder et al. 2016; Ciervo et al. 2016; Rianna et al. 2017a, 2017b), slope stability conditions are assessed through expeditious statistical approaches referring to rainfall thresholds, while physically based approaches are preferred in other cases. Finally, climate projections at 8km in the optimized configuration over Italy (Bucchignani et al. 2015) and the Zollo et al. (2014) configuration of COSMO_CLM model (the highest resolution currently available for Italy up to 2100) are used as inputs in the aforementioned case studies, while climate projections from the Euro-CORDEX multimodel ensemble (Giorgi et al., 2016) are adopted in Rianna et al. (2017b).

1.2 Object of the study

The present study focuses again on the Nocera Inferiore site, and also makes use, as will be discussed, of rainfall data from the sites of Gragnano and Castellammare di Stabia. The geographical collocation of the three towns in Italy and in the Campania region is illustrated in Fig. 1.

The study presents significant elements of novelty. For instance, through a Bayesian approach, it characterizes precipitation values cumulated on two time windows as proxies for the triggering of landslides affecting pyroclastic covers in the Monti Lattari mountain chain. The resulting quantitative model returns temporal variations in triggering probability, thus accounting for the effect of climate change on rainfall trends. Uncertainties in variations in rainfall patterns are taken into account recurring to the EURO-CORDEX ensemble. Projections provided by climate simulations are bias-adjusted, allowing the comparison with available physically-based rainfall thresholds while adding further assumptions and uncertainties in simulation chains. Landslide runout is also investigated probabilistically through a frequentist estimate of reach probability performed in a GIS environment, thus allowing the seamless mapping of landslide hazard under current and future climate change scenarios.

2 Description and modelling of the study area

2.1 Geographic and geomorphological description

Most of the territory of the Nocera Inferiore municipality belongs geomorphologically to the Sarno river valley. The most urbanized area of the town is located at the toe of the northern slopes of the Mount Albino relief, pertaining to the Monti Lattari chain (Fig. 2, sector A); other more sparsely populated areas are located at the foot of the Torricchio hills (Fig. 2, sector B). These reliefs are constituted by carbonate rocks covered by air-fall pyroclastic deposits originated from volcanic eruptions (Somma-Vesuvio complex) during the last 10,000 years (Pagano et al. 2010). Such covers in loose pyroclastic soils have been historically affected by multiple types of flow-like rainfall-induced landslides; among the most relevant events: Gragnano, 1997; Sarno & Quindici, 1998; Nocera, 2005; Ischia, 2006 (moreover, see Table 2 for a complete list of events affecting the area investigated in the work during 1960-2015 time span), including: (a) hyper-concentrated flows, which are generally triggered by washing away and/or progressive erosive processes along rills and inter-rill areas; (b) channelized debris flows, which can be generated by slope failure in ZOB areas (Dietrich et al. 1986; Cascini et al. 2008); and (c) un-channelized debris flows, which are locally triggered on open-slopes areas propagating as debris avalanches. The latter type characterized the most recent event which affected the city in March 2005, causing three fatalities and extensive damage to buildings and infrastructures (Pagano et al. 2010; Rianna et al. 2014). This study focuses specifically on a section of the Autostrada A3 "Salerno-Napoli" motorway, which runs across the toe of the Monte Albino relief as shown in Fig. 3.

Nat. Hazards Earth Syst. Sci. Discuss., https://doi.org/10.5194/nhess-2017-416
Manuscript under review for journal Nat. Hazards Earth Syst. Sci.
Discussion started: 5 December 2017

Natural Hazards and Earth System Sciences Discussions

3 Method of analysis

The study is conducted by coupling mathematical software with GIS in order to obtain spatially referenced estimates and allow mapping of hazard. The study area was modelled into the GIS software through a digital terrain model (DTM) having a resolution of 15x15 m. The original resolution adopted in the Regione Campania ORCA project (2004) was 5x5 m. A variety of DTM resolutions were tested for the case study. The adopted resolution proved to be sufficient to adequately represent the surface morphology and landslide runout as detailed in Section 6. Hazard is estimated quantitatively for each cell of the GIS-generated grid through the following model:

$$H = P_T \cdot P_R \quad (1)$$

in which P_T is the probability of landslide triggering, and P_R is the reach probability for the cell. It should be noted that the probability of triggering is related to rainfall parameters and, thus, is assumed to be uniform for the entire area, while reach probability depends on geomorphological factors, and is thus cell-specific and spatially variable within the area.

The study is conducted according to a modular approach initially involving the disjoint estimation of triggering probability (including its temporal variation) as described in Sec. 5, and reach probability, as detailed in Sec. 6. Subsequently, hazard is calculated using the model described above. The operational flowchart of the study is shown in Fig. 4. Source datasets are presented in Sec. 4.

4 Source datasets

4.1 Observed precipitation data

Observed datasets are used to identify time windows used as proxies for landslide triggering, to calibrate the Bayesian approach (see Sec. 5) and finally data from the Nocera Inferiore station are used to bias adjustment of climate projections (see Sec. 6).

Although the study is focuses on Nocera Inferiore landslide events, data from the neighbouring towns of Gragnano and Castellammare di Stabia are considered in order to increase the size of the event database, thus increasing the statistical significance of the approach. At both sites, landslide events affecting pyroclastic covers were observed to be very similar to those of the Nocera Inferiore slopes (De Vita & Piscopo 2002) as described in Sec. 4.2.

The dataset related to daily precipitation spans across the time window January 01, 1960- December 31, 2015. Unfortunately, for the three towns, no weather stations were in operation throughout the entire period. Consequently, the dataset is reconstructed by merging data provided by different weather stations. Prior to 1999, the network of monitoring stations was managed by Servizio Idrografico e Mareografico Nazionale (SIMN, Hydrographic and Tidal National Service) network at national level. In that period, the selected reference weather station is that located within the town and identified with the town's name as can be found in the SIMN yearbooks. Subsequently, the management was delegated to regional level, with the Regional Civil Protection managing the dataset for the Campania region. Since 1999, the reference weather stations are selected among those adopted for the towns in Regional Early Warning Systems against geological and hydrological hazards (Sistema

di Allertamento Regionale per il rischio idrogeologico e idraulico ai fini di protezione civile, 2005). Checks for the homogeneity of time series and for the unwarranted presence of breakpoints between the two periods were carried out for this study through the Pettitt (1979) and CUSUM (CUmulative SUM) (Smadi & Zghoul 2006) tests. Source weather stations, location, installation time and main (i.e., at least four months in a year) out-of-use periods are reported in Table 1.

4.2 Landslide inventory

The inventory of landslide events was compiled using three main references: Vallario (2000), De Vita & Piscopo (2002) and, for the more recent events, the "Event Reports" drafted by the Regional Civil Protection. It is worth recalling that only events affecting pyroclastic covers have been considered and included in the dataset. Sixteen events were observed in the period 1960-2015; these are reported in Table 2.

4.3 Climate projections

Climate projections for Nocera Inferiore were conducted as a preliminary step to the quantitative characterization of the temporal evolution of triggering probability as detailed in Sec. 5. The adopted simulation chain includes several elements. Firstly, scenarios about future variations in the concentrations of atmospheric gases inducing climate alterations are assessed through socio-economic approaches including demographic trends and land use changes. IPCC (Intergovernmental Panel on Climate Change) defined Reference Concentration Pathways (RCP) in terms of increases in radiative forcing in the year 2100 (compared to preindustrial era) of about 2.6, 4.5, 6 and 8.5 W/m^2. Such scenarios force Global Climate Models (GCM). These are recognized to reliably represent the main features of the global atmospheric circulation, but fail to reproduce weather conditions at temporal and spatial scales of relevance for assessing impacts at regional/local scale. In order to bridge such gap, GCMs are usually downscaled through Regional Climate Models (RCMs). These are climate models nested on GCMs, from which they retrieve initial and boundary conditions, but which work at higher resolution (including a non-hydrostatic formulation) on limited area. The dynamic downscaling from GCMs to RCMs allows a better representation of surface features (orography, land cover, etc.) and of associated atmospheric dynamics (e.g., convective processes). Nevertheless, persisting biases can hinder the quantitative assessment of local impacts.

In order to cope with such shortcomings, a number of strategies can be adopted. For instance, to characterize uncertainty associated to future projections, climate multi-models ensemble can be utilized where different combinations of GCM and RCM run on fixed grid and domain. Furthermore, statistical approaches (e.g., Maraun 2013; Villani et al. 2015; Lafon et al. 2013) can be pursued to reduce biases assumed as systematic in simulations. More specifically, quantile mapping approaches have been applied with satisfactory results in recent years for different impact studies. In these applications, the correction is performed as to ensure that "a quantile of the present day simulated distribution is replaced by the same quantile of the present-day observed distribution" (Maraun 2013). However, limitations and assumptions associated to these approaches should be clear to practitioners (Ehret 2012; Maraun & Widmann, 2015).

Nat. Hazards Earth Syst. Sci. Discuss., https://doi.org/10.5194/nhess-2017-416
Manuscript under review for journal Nat. Hazards Earth Syst. Sci.
Discussion started: 5 December 2017

Natural Hazards and Earth System Sciences Discussions

In the present study, climate simulations included in EURO-CORDEX multi-model ensemble at 0.11' (approximately 12 km) are considered under the RCP4.5 and RCP8.5 scenarios as described in Table 3. Climate simulations are bias-adjusted through an empirical quantile mapping approach (Gudmundson et al. 2012) using data from Nocera Inferiore weather stations from the period 1981-2010.

5 Calculation of triggering probability

Landslide triggering probability was estimated quantitatively as a function of two cumulative rainfall thresholds; namely, the 1-day rainfall β_{01} and the 59-day rainfall β_{59}. Such cumulative parameters were calculated using a moving window procedure for and associated with each day from January 01, 1960 to December 31, 2015 from the observed precipitation data described in Sec. 4.1. The number of landslide events observed for each day at the Nocera Inferiore, Gragnano and Castellammare di Stabia as reported in the landslide inventory was associated with the rainfall data. Fig. 5 plots the pairs of β_{01} and β_{59} recorded daily in the period 1960-2015, along with the indication of occurrence (by site) or non-occurrence of landslide events.

The probability of landslide triggering is given by

$$P_T = \sum_{i=1}^{N_{\beta 01}} \sum_{j=1}^{N_{\beta 59}} \left[P\left(T|\beta_{01}^{(i)}, \beta_{59}^{(j)}\right) \cdot P\left(\beta_{01}^{(i)}, \beta_{59}^{(j)}\right) \right] \quad (2)$$

in which

$\beta_{01}^{(i)}$	i-th value of cumulative rainfall β_{01} (i=1,…, $N_{\beta 01}$)
$\beta_{59}^{(j)}$	j-th value of cumulative rainfall β_{59} (j=1,…,$N_{\beta 59}$)
$P\left(T|\beta_{01}^{(i)}, \beta_{59}^{(j)}\right)$	conditional probability of triggering of a landslide given the simultaneous occurrence of $\beta_{01}^{(i)}$ and $\beta_{59}^{(j)}$
$P\left(\beta_{01}^{(i)}, \beta_{59}^{(j)}\right)$	joint probability of simultaneous occurrence of $\beta_{01}^{(i)}$ and $\beta_{59}^{(j)}$

The conditional probability of triggering of a landslide given the simultaneous occurrence of $R_{01}^{(i)}$ and $R_{59}^{(j)}$ is obtained from the Bayesian approach is estimated using a Bayesian approach as suggested by Berti et al. (2012). The procedure refers to Bayes' theorem, formulated as follows:

$$P\left(T|\beta_{01}^{(i)}, \beta_{59}^{(j)}\right) = \frac{P\left(\beta_{01}^{(i)}, \beta_{59}^{(j)}|T\right) \cdot P(T)}{P\left(\beta_{01}^{(i)}, \beta_{59}^{(j)}\right)} \quad (3)$$

in which, in Bayesian glossary, $P\left(\beta_{01}^{(i)}, \beta_{59}^{(j)}|T\right)$ is the likelihood, i.e., the conditional joint probability of simultaneous occurrence of $\beta_{01}^{(i)}$ and $\beta_{59}^{(j)}$ if a landslide is triggered in the reference area; and $P(T)$ is the prior probability, i.e., the probability of triggering of a landslide in the reference area, regardless of the magnitude of β_{01} and β_{59}.

Let

N_β	total number of rainfall events recorded during a given reference time period

Nat. Hazards Earth Syst. Sci. Discuss., https://doi.org/10.5194/nhess-2017-416
Manuscript under review for journal Nat. Hazards Earth Syst. Sci.
Discussion started: 5 December 2017

Natural Hazards and Earth System Sciences Discussions

N_L total number of landslides occurred during the given reference time period

$N_{\beta_{01}^{(i)}}$ number of rainfall events of a given magnitude of β_{01} recorded during the given time reference

$N_{\beta_{59}^{(j)}}$ number of rainfall events of a given magnitude of β_{59} recorded during the given time reference

The likelihood can be calculated as the product of the marginal conditional probabilities of attainment of $\beta_{01}^{(i)}$ and $\beta_{59}^{(j)}$ given the occurrence of a landslide:

$$P\left(\beta_{01}^{(i)}, \beta_{59}^{(j)} | T\right) = P\left(\beta_{01}^{(i)} | T\right) \cdot P\left(\beta_{59}^{(j)} | T\right) \quad (4)$$

The above Bayesian probabilities can be computed in terms of relative frequencies as follows:

$$P(T) = \frac{N_L}{N_\beta} \quad (5)$$

$$P\left(\beta_{01}^{(i)} | T\right) = \frac{N_{\beta_{01}^{(i)}|T}}{N_L} \quad (6)$$

$$P\left(\beta_{59}^{(j)} | T\right) = \frac{N_{\beta_{59}^{(j)}|T}}{N_L} \quad (7)$$

in which

$N_{\beta_{01}^{(i)}|T}$ number of rainfall events of magnitude at least $\beta_{01}^{(i)}$ recorded during the given time reference and which resulted in the triggering of landslides

$N_{\beta_{59}^{(j)}|T}$ number of rainfall events of magnitude at least $\beta_{59}^{(j)}$ recorded during the given time reference and which resulted in the triggering of landslides

The joint probability of simultaneous occurrence of $\beta_{01}^{(i)}$ and $\beta_{59}^{(j)}$ is obtained as the frequentist ratio of the number of days in which the simultaneous occurrence of $\beta_{01}^{(i)}$ and $\beta_{59}^{(j)}$ was recorded to the total number of days for which observations at the rain gauges are available.

Figure 6 plots landslide triggering probability as a function of 1-day and 59-days cumulative rainfall, as estimated through the Bayesian approach. Figure 7 plots the temporal variation of triggering probability for 30-year periods from 1981-2010 to 2071-2100 and for the RCP4.5 and RCP 8.5 scenarios. More specifically, Fig. 7a shows the temporal variation of triggering probability for scenario RCP4.5 for each of the 10 CORDEX models, along with the sample mean, minimum and maximum. Figure 7b shows the corresponding data for scenario RCP8.5. Figure 7c plots the outputs of both scenarios, while Fig. 7d plots the temporal variation of the sample coefficient of variation for both-scenarios. Such statistic is given by the ratio of the sample standard deviation and the sample mean, and describes quantitatively the scatter among CORDEX model outputs.

For the RCP4.5 scenario, considering the running 30-year averages, all available projections predict a moderate increase, with few differences. In this regard, a higher spread among the models is recognizable at the middle of the XXI century. Such increased spread is mainly due to the outputs of two models constantly representing, respectively, the upper and bottom boundaries of the ensemble throughout the entire investigated period. Nevertheless, the increase in mean terms worth about

35-40% at the end of the century. It is interesting to note how, in average terms, minor differences are recognizable between the two scenarios with the largest variations in 2041-2080 time span where the triggering probability is slightly higher under the more pessimistic scenario. Also in terms of coefficient of variations, in the first part of the century, slight differences are recognizable under the two scenarios; however, also in terms of concentrations of gases (green house of chemically active), higher differences arise in the second part of the century.

In this perspective, it is interesting to note how in the end of the century differences nullify probably due to joint effect of contrasting trends in proxies estimated, in average terms, under RCP8.5 (increase in values of β_{01} and reduction in β_{59}). To this aim, it is worth to note that the effects of evapotranspiration, reducing the soil wetting and that could have a significant role because of increased warming, are neglected in the developed framework. On the other hand, in this case, the projections returned by a model included in the ensemble significantly differ from the other ones with P_T values attaining about $3x10^{-3}$ against a mean value of about $1.5x10^{-3}$. In this way, the coefficient of variation is significantly higher than this estimated under RCP4.5. However, several assumptions and constraints affect retrieved findings; among the other ones, land use/land cover features are assumed not significantly affecting proxy values during the calibration and future period; nevertheless, local conditions could substantially modify the landslide susceptibility (e.g. fires destroying vegetation) altering, at the same time, exposure (also assumed constant during the entire period).

6 Estimation of reach probability

Investigation of the spatial variability of landslide hazard entails the modelling of its downslope propagation (runout). Reach probability is the probability (from 0: certainty of no reach to 1: certainty of reach) of each point in the spatial domain being affected by the landslide during the runout process. Several morphological, empirical and physically-based approaches are available for quantitative runout analysis (Hürlimann et al. 2008); each of these may present advantages or weaknesses in relation to site- and/or phenomenon-specific attributes, data availability and scale of the analysis. Consistently with the methods previously used to define triggering-rainfall scenarios, the approach used to define downslope runout scenarios is based on an algorithm involving stochastic modelling.

6.1 Reach probability calculation method

Landslide reach probability was computed spatially using Flow-R, a DTM-based distributed empirical model developed in the Matlab® environment (Horton et al. 2013). The flow-slide spreading is controlled by a flow direction algorithm that reproduces flow paths (Holmgren 1994) and by a persistence function to consider inertia and abruptness in change of the flow direction (Gamma 2000). The flow direction algorithm proposed by Holmgren (1994), in the setting used in this study (x=1, see Eq. (3) in Horton et al. 2013) is similar to the multiple D8 of Quinn et al. (1991, 1995). The multiple D8 distributes the flow to all neighbouring downslope cells weighted according to slope. The algorithm tends to produce more realistic looking spatial patterns than the simple D8 algorithm by avoiding concentration to distinct lines (Seibert & McGlynn 2007). The maximum

Nat. Hazards Earth Syst. Sci. Discuss., https://doi.org/10.5194/nhess-2017-416
Manuscript under review for journal Nat. Hazards Earth Syst. Sci.
Discussion started: 5 December 2017

possible runout distances are computed by means a *simplified frictional-limited model* based on a unitary energy balance (Horton et al. 2013).

One-run propagation simulation provides possible flow-paths generated from previously identified triggering/source areas. In this work, source areas were identified by means of the official geo-morphological map of the "Campania Centrale" River Basin Authority (PSAI 2015) and coincide with the union of the "zero order basin" (ZOB) and current "niche/failure" areas. This hypothesis is in accordance with the requirement of consistency with accounts of historical events and with the aim to consider the most pessimistic possible triggering scenarios (i.e., those with maximum mass potential energy).

The reach probability for any given cell P_R is calculated by the following equation:

$$P_R = \frac{p_u^{fd} p_u^p}{\sum_{v=1}^{8} p_v^{fd} p_v^p} p_0 \quad (8)$$

where u and v are the flow directions; p_u is the probability value in the u-th direction; p_u^{fd} is the flow proportion according to the flow direction algorithm; p_u^p is the flow proportion according to the persistence function; and p_0 is the probability determined in the previous cell along the generic computed path. The values are subsequently normalized. Runout routing is stopped when: (1) the angle of the line connecting the source area to the most distant point reached by the flow-slide along the generic computed path is smaller than a predefined *angle of reach* (Corominas 1996); and (2) the velocity exceeds a user-fixed maximum value, or is below the value corresponding to the maximum energy lost due to friction along the path. The values which do not fit the above-mentioned requirements are redistributed among the active cells to ensure conservation of the total probability value.

6.2 Reach probability outputs

The propagation routine was applied to the DTM described in Sec. 3. An *angle of reach* of 4° was calibrated based on the geo-morphological information (i.e., the extension of the slope fan deposition) and the official hazard maps of the Landslide Risk Management Plan of the River Basin Authority (PSAI, 2015). Consistently with the mean values reported by the scientific literature (Faella & Nigro 2001; Revellino et al. 2004) for the same phenomena and in the same region, the maximum runout velocity was set at 10 m/s. Figure 8 illustrates the spatial distribution of reach probability at hillslope scale. Source areas are also indicated.

In this area, the highway runs mostly on a soil embankment. The road level is generally elevated with respect to the paths of the downslope flows. The propagation impacts the embankment and stops in front of - or laterally continues according to - the topographic information and the model setting. Differently, in some points, the highway runs approximately at the same level of the fans, thereby allowing the propagating flow to invade the road. In both cases, damage or disruptions may be caused to the infrastructure. In order to overcome this distinction and to cover both scenarios, only flow propagation to the upstream boundary of the infrastructure are considered in the study. An illustrative example is shown in the magnified focus area in Fig. 9. Due to the reasons mentioned above, the road surface is only partially affected by the flow-slides. Confining the study just

to a part of the infrastructure (e.g., from A to B), the runout values to be considered in the risk assessment should be taken along the section A-B (Fig. 10). Hazard can be calculated directly for a given year and RCP scenario by applying Eq. (1). The results shown in Fig. 10 attest for the marked spatial variability of reach probability (and, therefore, of hazard) along the investigated section of the A3 motorway infrastructure.

7 Concluding remarks

This paper has illustrated a methodology for the quantitative estimation of rainfall-induced landslide hazard. An example application of the proposed method was conducted for a short section of a motorway. Despite the limited extension of the study area, the results displayed a marked temporal and spatial variability of hazard. The temporal variability of hazard is a consequence of climate change as parameterized through quantitative projections for concentration scenarios RCP4.5 and RCP8.5. Significant temporal variability was predicted for both concentration scenarios. The considerable spatial variability resulting from the case study stems from the spatial variability of reach probability as modelled in the runout analysis.

The hazard outputs obtained by the method can be used directly in the quantitative estimation of landslide risk. The latter also requires the quantitative estimation of the vulnerability of human-valued assets (i.e., vehicles, persons, etc.) and the exposure (i.e., the number and/or degree of presence) of the assets themselves in the study area in a reference time period.

The quantitative estimates of hazard as obtained in this paper are pervaded by significant uncertainty. Among the main sources of uncertainty are the climate change projections, the runout model and the Bayesian model developed to quantify triggering probability. These uncertainties are epistemic in nature, as they stem from the inherent difficulty in compiling climate change projections, the inevitable degree of approximation and imperfection in runout modelling capabilities, the limited rainfall and landslide occurrence data used to develop triggering probability curves. As such, increased modelling capability and improved databases could reduce the magnitude of uncertainty associated with hazard estimation.

Notwithstanding the above uncertainties, the quantitative estimation and assessment of the spatial and temporal variability of hazard provide an important decision support tool in the disaster risk management cycle; specifically, in the planning and prioritization of hazard mitigation and risk mitigation measures. The availability of quantitative methods allows a more rational decision-making process in which the costs and effectiveness of risk mitigation can be compared and assessed in terms of convenience.

Acknowledgments

The research leading to these results has received funding from the European Union Seventh Framework Program (FP7/2007-2013) under grant agreement No. 606799. The support is gratefully acknowledged.

References

Berti, M., Martina, M.L.V., Franceschini, S., Pignone, S., Simoni, A. and Pizziolo, M.: Probabilistic rainfall thresholds for landslide occurrence using a Bayesian approach, Journal of Geophysical Research, 117, F04006, doi:10.1029/2012JF002367, 2012.

Beven, K. J.: EGU Leonardo Lecture: facets of hydrology – epistemic error, non- stationarity, likelihood, hypothesis testing, and communication, Hydrol. Sci. J., doi:10.1080/02626667.2015.1031761, 2015.

Beven, K. J., Aspinall, W. P., Bates, P. D., Borgomeo, E., Goda, K., Hall, J. W., Page, T., Phillips, J. C., Simpson, M., Smith, P. J., Wagener, T. and Watson, M.:Epistemic uncertainties and natural hazard risk assessment. 2. What should constitute good practice?, Nat. Hazards Earth Syst. Sci. Discuss., https://doi.org/10.5194/nhess-2017-251, 2017 (in review).

Bucchignani, E., Montesarchio, M., Zollo, A.L. and Mercogliano, P.:High-resolution climate simulations with COSMO-CLM over Italy: Performance evaluation and climate projections for the 21st century, Int. J. Climatol, doi:10.1002/joc.4379, 2015.

Cascini, L., Cuomo, S. and Guida, D.: Typical source areas of May 1998 flow-like mass movements in the Campania region, Southern Italy, Engineering Geology, 96(3), 107–125, 2008.

Chancel, L. and Piketty, T.: Carbon and inequality: from Kyoto to Paris. Trends in the global inequality of carbon emissions (1998-2013) & prospects for an equitable adaptation fund, Iddri & Paris School of Economics Report, 2015.

Ciervo, F., Rianna, G., Mercogliano, P. and Papa, M.N.: Effects of climate change on shallow landslides in a small coastal catchment in southern Italy, Landslides, doi:10.1007/s10346-016-0743-1, 2016.

Cooke, R. M.: Messaging climate change uncertainty, Nature Clim. Change, 5, 8–10, doi:10.1038/nclimate2466, 2014.

Corominas, J.: The angle of reach as a mobility index for small and large landslides, Canadian Geotechnical Journal, 33, 260–271. doi:10.1139/t96-130, 1996.

Cox, L.A.: Confronting deep uncertainties in risk analysis, Risk Analysis, 32(10), 1607–1629, 2012.

Damiano, E. and Mercogliano, P.: Potential effects of climate change on slope stability in unsaturated pyroclastic soils, In: Margottini C., Canuti P., Sassa K. (Eds) Book Series ‘‘Landslide Science and Practice’’, Vol. 4 ‘‘Global Environmental Change”, 4, 15–25, 2013.

De Vita, P. and Piscopo, V.: Influences of hydrological and hydrogeological conditions on debris flows in peri-Vesuvian hillslopes, Natural Hazards and Earth System Sciences, 2(1-2), 27–35, 2002.

Dietrich, W.E., Wilson, C.J. and Reneau, S.L.: Hollows, colluvium, and landslides in soil-mantled landscapes, Hillslope processes, 361-388, 1986.

Ehret, U., Zehe, E., Wulfmeyer, V., Warrach-Sagi, K. and Liebert, J.: HESS Opinions ‘should We Apply Bias Correction to Global and Regional Climate Model Data?’, Hydrology and Earth System Sciences, 16(9), 3391–3404, 2012.

Faella, C. and Nigro, E.: Effetti delle colate rapide sulle costruzioni. Parte Seconda: Valutazione della velocita` di impatto, Forum per il Rischio Idrogeologico ‘‘Fenomeni di colata rapida di fango nel Maggio ’98’’, Napoli, 22 giugno 2001, 113–125, 2001.

Gamma, P.: Ein Murgang-Simulationsprogramm zur Gefahrenzonierung, Geographisches Institut der Universität Bern, 2000.

Gariano, S.L. and Guzzetti, F.: Landslides in a changing climate, Earth-Sci. Rev., doi:10.1016/j.earscirev.2016.08.011, 2016.

Giorgi, F., and Gutowski, W.J.: Coordinated Experiments for Projections of Regional Climate Change, Current Climate Change Reports, 2016.

Gudmundsson, L., Bremnes, J.B., Haugen, J.E. and Engen-Skaugen, T.: Technical Note: Downscaling RCM precipitation to the station scale using statistical transformations: a comparison of methods, Hydrology and Earth System Sciences, 16(9), 3383–3390, 2012.

Hallegatte, S., Shah, A., Lempert, R., Brown, C. and Gill, S.: Investment decision making under deep uncertainty: application to climate change, Policy Research Working Paper 6193, 41, 2012.

Holmgren P.: Multiple flow direction algorithm for runoff modeling in grid based elevation models: an empirical evaluation, Hydrological Processes, 8, 327– 334, 1994.

Horton, P., Jaboyedoff, M., Rudaz, B.E.A. and Zimmermann, M.: Flow-R, a model for susceptibility mapping of debris flows and other gravitational hazards at a regional scale, Natural Hazards and Earth System Sciences, 13(4), 869-885, 2013.

Hürlimann, M., Rickenmann, D., Medina, V. and Bateman, A.: Evaluation of approaches to calculate debris-flow parameters for hazard assessment, Engineering Geology, 102(3), 152-163, 2008.

Koutsoyiannis, D. and Montanari, A.: Statistical analysis of hydroclimatic time series: Uncertainty and insights, Water Resour. Res., 43, W05429, doi:10.1029/2006WR005592, 2007.

Lafon, T., Dadson, S., Buys, G. and Prudhomme, C.: Bias correction of daily precipitation simulated by a regional climate model: a comparison of methods, International Journal of Climatology 33(6), 1367–1381, 2013.

Maraun, D.: Bias correction, quantile mapping, and downscaling: revisiting the inflation issue, Journal of Climate, 2137–2143, 2013.

Maraun, D., and Widmann, M.: The Representation of Location by a Regional Climate Model in Complex Terrain, Hydrology and Earth System Sciences, 19(8), 3449–3456, 2015.

Pagano, L., Picarelli, L., Rianna, G., and Urciuoli, G.: A simple numerical procedure for timely prediction of precipitation-induced landslides in unsaturated pyroclastic soils, Landslides 7(3), 273–89, 2010.

Pettitt, A.N.: A non-parametric approach to the change point problem, Applied Statistics, 28(2), 126-135, 1979.

Picarelli L., Santo, A., Di Crescenzo, G. and Olivares, L.: Macro-zoning of areas susceptible to flowslide in pyroclastic soils in Campania Region, In: Chen Z, Zhang J, Li Z, Wu F, Ho K (Eds.), Proc. 10th Int. Symp. on Landslides. Xi'an, 2, 1951-1958, Taylor & Francis, London, 2008.

Quinn, P. F., Beven, K. J., Chevallier, P. and Planchon, O.: The prediction of hillslope flowpaths for distributed modelling using digital terrain models, Hydrological Processes, 5, 59–80, 1991.

Quinn, P. F., Beven, K. J. and Lamb, R.: The ln(a/tanβ) index: How to calculate it and how to use it within the TOPMODEL framework, Hydrological Processes, 9, 161–182, 1995.

Reder, A., Rianna, G., Mercogliano, P. and Pagano, L.: Assessing the Potential Effects of Climate Changes on Landslide Phenomena Affecting Pyroclastic Covers in Nocera Area (Southern Italy), Procedia Earth Planet. Sci., 16, 166–176, doi:10.1016/j.proeps.2016.10.018, 2016.

Revellino, P., Hungr, O., Guadagno, F.M. and Evans, S.G.: Velocity and runout simulation of destructive debris flows and debris avalanches in pyroclastic deposits, Campania region, Italy, Env Geol., 45, 295, https://doi.org/10.1007/s00254-003-0885-z, 2004.

Rianna, G., Pagano, L. and Urciuoli, G.: Rainfall Patterns Triggering Shallow Flowslides in Pyroclastic Soils, Engineering Geology, 174, 22–35, http://dx.doi.org/10.1016/j.enggeo.2014.03.004, 2014.

Rianna, G., Comegna, L., Mercogliano, P. and Picarelli, L.: Potential effects of climate changes on soil–Atmosphere interaction and landslide hazard, Nat. Hazards, doi:10.1007/s11069-016-2481-z, 2016.

Rianna, G., Reder, A., Mercogliano, P. and Pagano, L.: Evaluation of variations in frequency of landslide events affecting pyroclastic covers in the Campania region under the effect of climate changes, Hydrology, 4, 34, 2017a.

Rianna, G., Reder, A., Villani, V. and Mercogliano, P.: Variations in landslide frequency due to climate changes through high resolution Euro-CORDEX Ensemble, Proc. IV World Landslide Forum, 237–42. http://link.springer.com/10.1007/978-3-319-53485-5, 2017b.

Seibert, J. and McGlynn, B. L.: A new triangular multiple flow direction algorithm for computing upslope areas from gridded digital elevation models". Water Resources Research, 43(4), 2007.

Seneviratne, S.I., Nicholls, N., Easterling, D., Goodess, C.M., Kanae, S., Kossin, J., Luo, Y., Marengo, J., McInnes, K., Rahimi, M., Reichstein, M., Sorteberg, A., Vera, C. and Zhang, X.: Changes in climate extremes and their impacts on the natural physical environment, In: Managing the Risks of Extreme Events and Disasters to Advance Climate Change Adaptation [Field, C.B., V. Barros, T.F. Stocker, D. Qin, D.J. Dokken, K.L. Ebi, M.D. Mastrandrea, K.J. Mach, G.-K. Plattner, S.K. Allen, M. Tignor, and P.M. Midgley (eds.)]. A Special Report of Working Groups I and II of the Intergovernmental Panel on Climate Change (IPCC), Cambridge University Press, Cambridge, UK, and New York, NY, USA, 109-230, 2012.

Smadi, M.M. and Zghoul, A.: A sudden change in rainfall characteristics in Amman, Jordan during the mid-1950s, American Journal of Environmental Sciences, 2(3), 84-91, 2006.

Stein, S. and Stein, J.L.: Shallow Versus Deep Uncertainties in Natural Hazard Assessments, Eos, Transactions American Geophysical Union 94(14), 133–34. http://doi.wiley.com/10.1002/2013EO140001, 2013.

Stern, N.: The Stern Review on the Economics of Climate Change ISBN number: 0-521-70080-9, 2006.

Vallario, A.: Il dissesto idrogeologico in Campania, CUEN, 2000.

Villani, V., Rianna, G., Mercogliano, P. and Zollo, A.L.: Statistical approaches versus weather generator to downscale RCM outputs to slope scale for stability assessment: a comparison of performances, Electronic Journal of Geotechnical Engineering, 20(4), 1495–1515, 2015.

Wilby, R. L. and Dessai, S.: Robust Adaptation to Climate Change, Weather, 65(7), 176–80, 2010.

Nat. Hazards Earth Syst. Sci. Discuss., https://doi.org/10.5194/nhess-2017-416
Manuscript under review for journal Nat. Hazards Earth Syst. Sci.
Discussion started: 5 December 2017

Natural Hazards and Earth System Sciences
Discussions

Table 1. Weather stations used in the compilation of datasets for Nocera Inferiore, Gragnano and Castellammare di Stabia: location, installation time and main out-of-use periods

Town	Weather station (1060-1999)	Installation and main out-of-use periods	Weather Station (2000-2015)	Installation and main out-of-use periods
Nocera Inferiore	Nocera Inferiore (61 m asl) 40° 45’ 0’’ N 14° 38’ 9’’ E	Since 1899 1964,1965,1967, 1981,1982	Tramonti (422 m asl) 40° 42’ 14” N 14° 38’ 49” E	Since February 2002 2000,2001
Gragnano	Gragnano (173 m asl) 40° 40’ 59’’N 14° 31’ 9’’ E	Since 1921	Gragnano_2 (195 m asl) 40° 41’ 15” N 14° 31’ 38” E	Since November 2001 2000,2001
Castellammare di Stabia	Castellammare di Stabia (18 m asl) 14.486111 40.7	Since 1929 1964,1965,1966	Pimonte (437 m asl) 40° 40’ 27” N 14° 30’ 17” E	Since October 2000 2000

Nat. Hazards Earth Syst. Sci. Discuss., https://doi.org/10.5194/nhess-2017-416
Manuscript under review for journal Nat. Hazards Earth Syst. Sci.
Discussion started: 5 December 2017

Natural Hazards and Earth System Sciences
Discussions

Table 2. Landslide events affecting pyroclastic covers in Nocera Inferiore, Gragnano and Castellammare di Stabia in the period 1960-2015

Nocera Inferiore	Gragnano	Castellammare di Stabia
8 December 1960	17 February 1963	17 February 1963
4 November 1961	2 January 1971	17 November 1985
6 March 1972	21 January 1971	23 February 1987
10 January 1997	22 February 1986	10 November 1987
4 March 2005	10 January 1997	11 January 1997
	March 2005	

Nat. Hazards Earth Syst. Sci. Discuss., https://doi.org/10.5194/nhess-2017-416
Manuscript under review for journal Nat. Hazards Earth Syst. Sci.
Discussion started: 5 December 2017

Natural Hazards and Earth System Sciences
Discussions

Table 3. Available Euro-CORDEX simulations at a 0.11º resolution (~12km) over Europe, providing institutions, GCM and RCMs

Code	Institution	GCM	RCM
1	CLMcom	CNRM-CM5_r1i1p1	CCLM4-8-17_v1
2	CLmcom	EC-EARTH_r12i1p1	CCLM4-8-17_v1
3	CLMcom	MPI-ESM-LR_r1i1p1	CCLM4-8-17_v1
4	DMI	EC-EARTH_r3i1p1	HIRHAM5_v1
5	KNMI	EC-EARTH_r1i1p1	RACMO22E_v1
6	IPSL-INERIS	IPSL-CM5A-MR_r1i1p1	WRF331F_v1
7	SMHI	CNRM-CM5_r1i1p1	RCA4_v1
8	SMHI	EC-EARTH_r12i1p1	RCA4_v1
9	SMHI	MPI-ESM-LR_r1i1p1	RCA4_v1
10	SMHI	IPSL-CM5A-MR_r1i1p1	RCA4_v1

Nat. Hazards Earth Syst. Sci. Discuss., https://doi.org/10.5194/nhess-2017-416
Manuscript under review for journal Nat. Hazards Earth Syst. Sci.
Discussion started: 5 December 2017

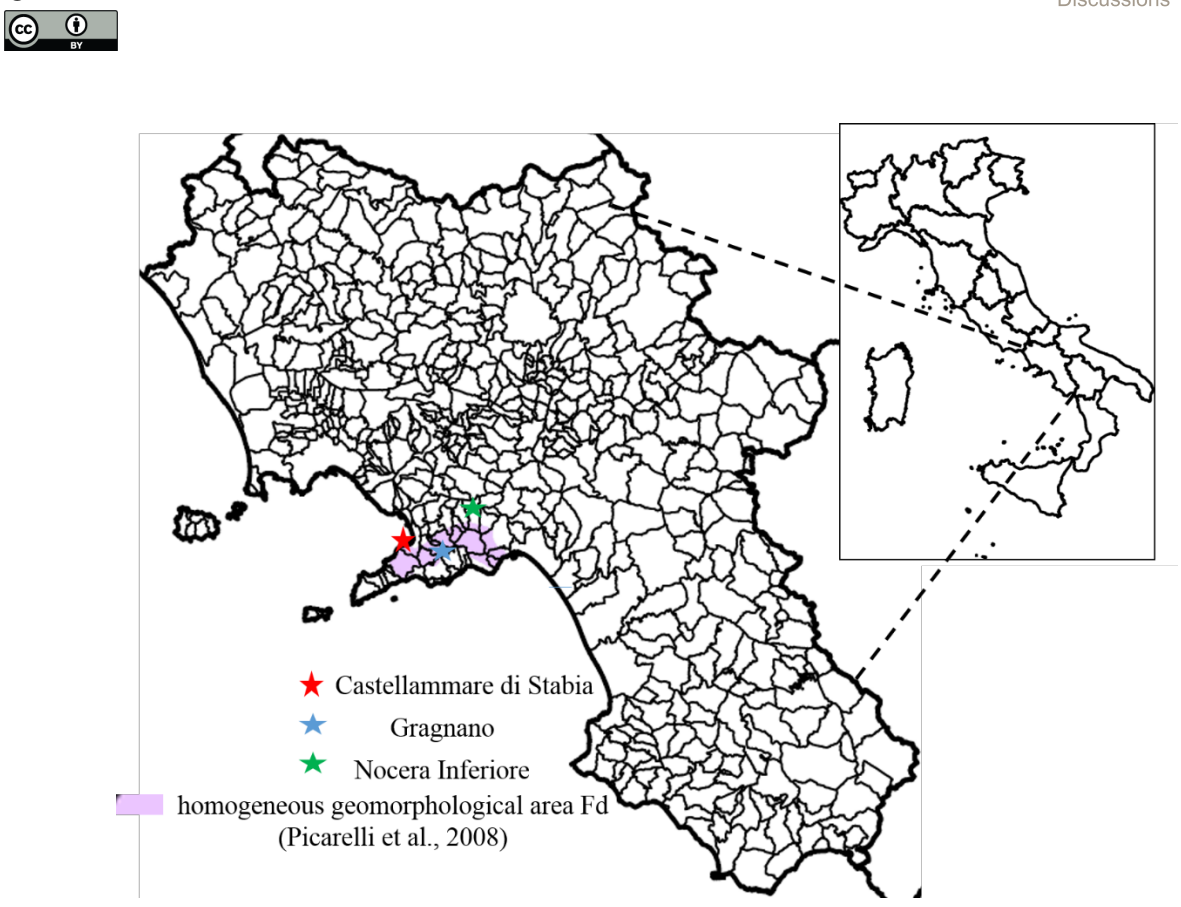

Figure 1. Identification of the three towns considered in the study

Nat. Hazards Earth Syst. Sci. Discuss., https://doi.org/10.5194/nhess-2017-416
Manuscript under review for journal Nat. Hazards Earth Syst. Sci.
Discussion started: 5 December 2017

Natural Hazards and Earth System Sciences
Discussions

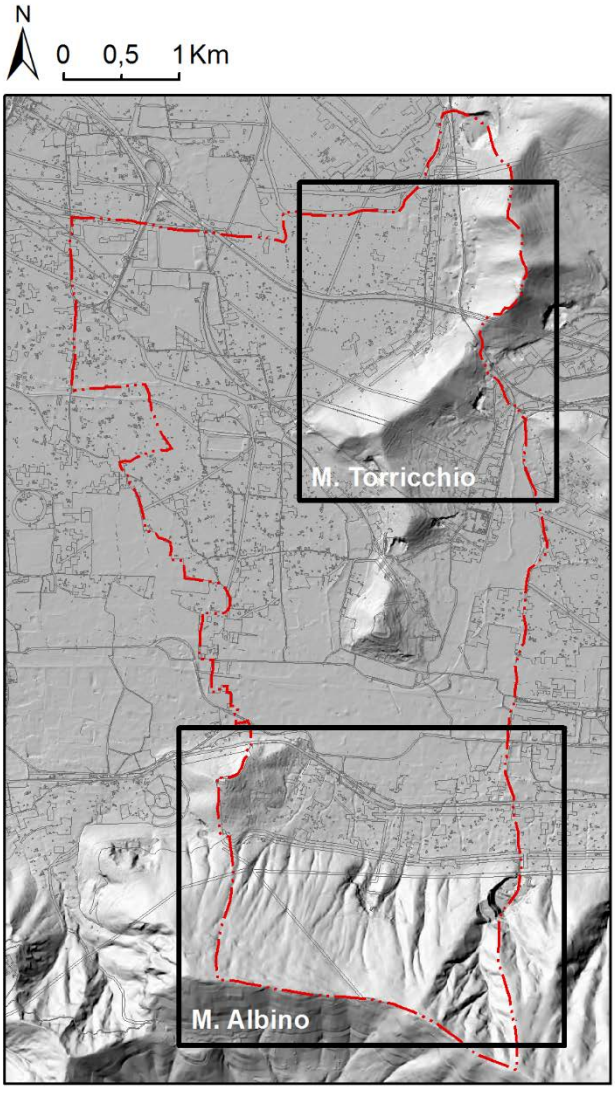

Figure 2. Geomorphologic setting and administrative boundaries of the Nocera Inferiore municipality

Nat. Hazards Earth Syst. Sci. Discuss., https://doi.org/10.5194/nhess-2017-416
Manuscript under review for journal Nat. Hazards Earth Syst. Sci.
Discussion started: 5 December 2017

Natural Hazards and Earth System Sciences
Discussions

Figure 3. Infrastructure-scale view of the study area

Nat. Hazards Earth Syst. Sci. Discuss., https://doi.org/10.5194/nhess-2017-416
Manuscript under review for journal Nat. Hazards Earth Syst. Sci.
Discussion started: 5 December 2017

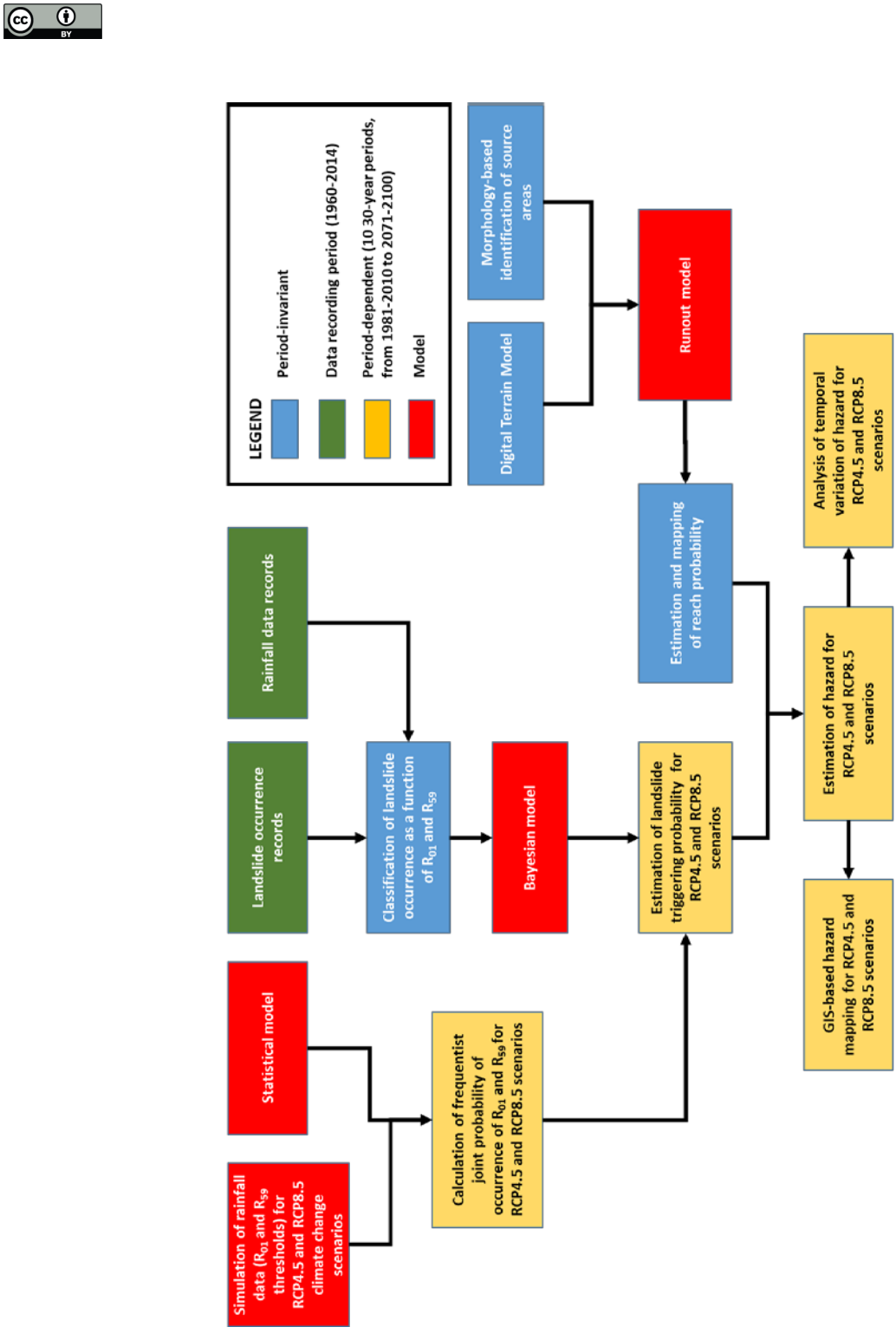

Figure 4. Operational flowchart of the study

Nat. Hazards Earth Syst. Sci. Discuss., https://doi.org/10.5194/nhess-2017-416
Manuscript under review for journal Nat. Hazards Earth Syst. Sci.
Discussion started: 5 December 2017

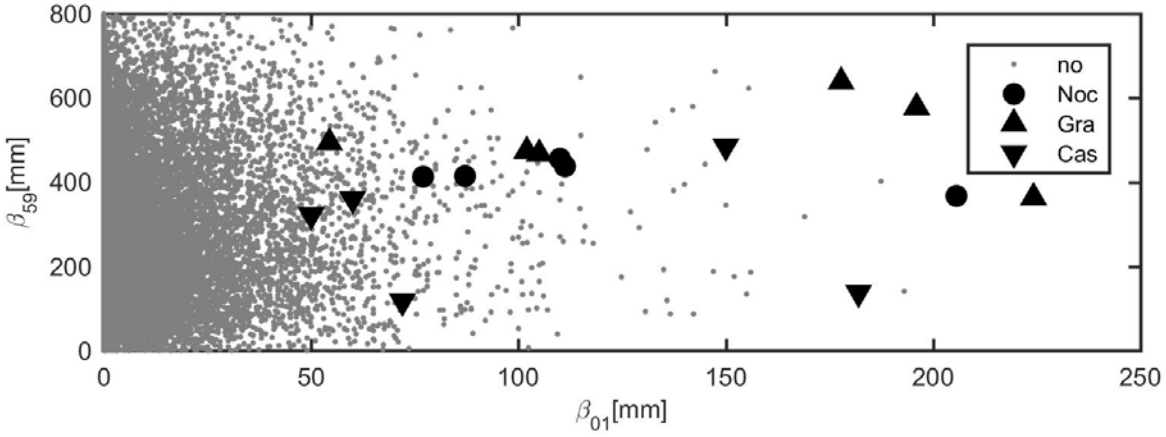

Figure 5. Pairs of β_{01} and β_{59} recorded daily in the period 1960-2015, with occurrence (by site) or non-occurrence of landslide events

Nat. Hazards Earth Syst. Sci. Discuss., https://doi.org/10.5194/nhess-2017-416
Manuscript under review for journal Nat. Hazards Earth Syst. Sci.
Discussion started: 5 December 2017

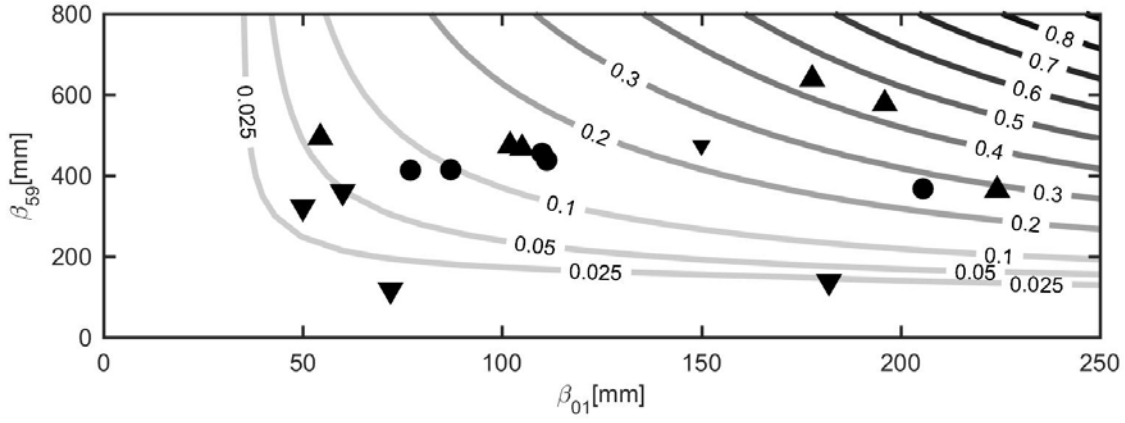

Figure 6. Landslide triggering probability as a function of 1-day and 59-days cumulative rainfall

Nat. Hazards Earth Syst. Sci. Discuss., https://doi.org/10.5194/nhess-2017-416
Manuscript under review for journal Nat. Hazards Earth Syst. Sci.
Discussion started: 5 December 2017

Natural Hazards and Earth System Sciences
Discussions

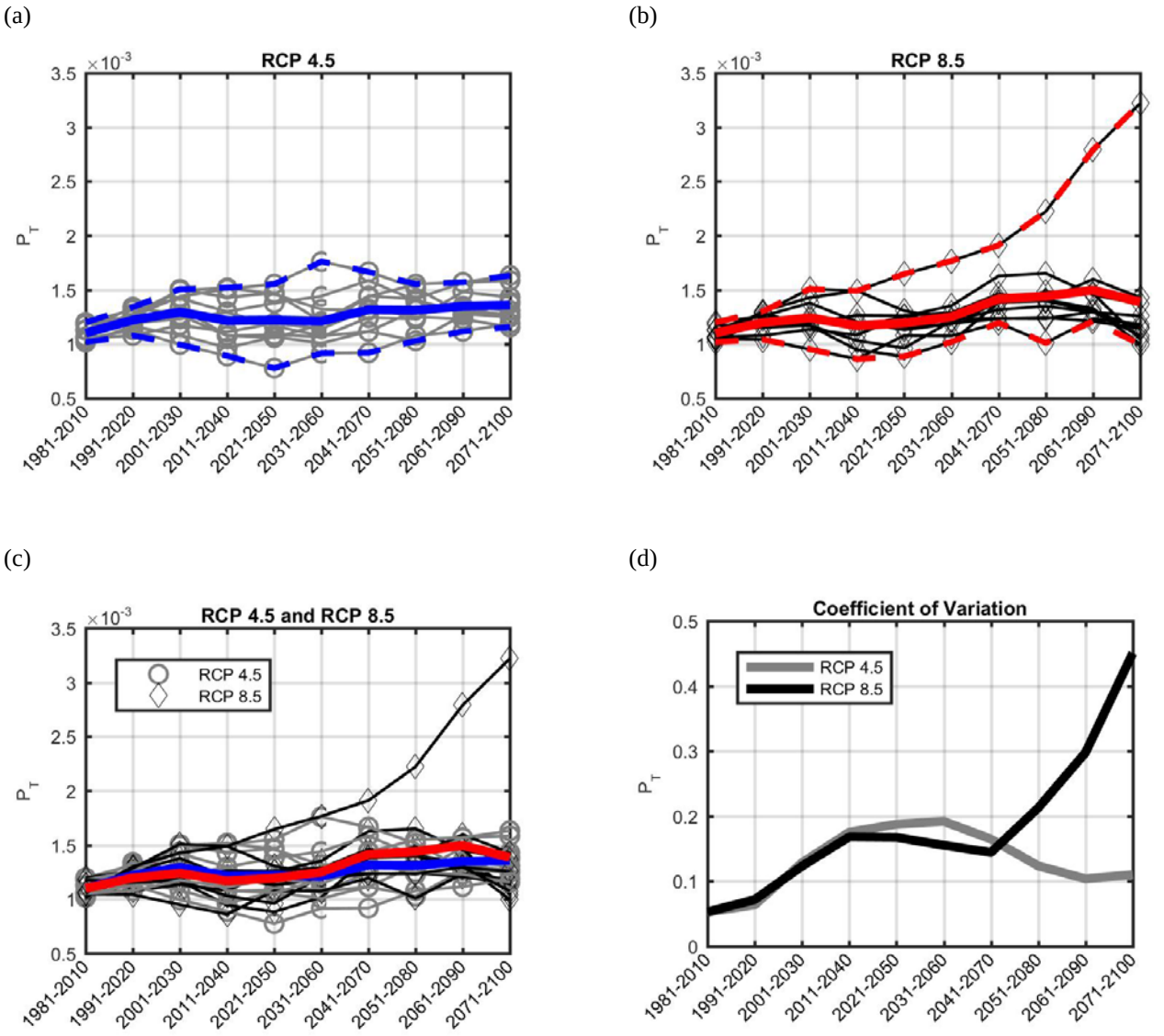

Figure 7. Triggering probability for 30-year periods from 1981-2010 to 2071-2100: (a) model outputs, mean and maximum-minimum envelopes for the RCP4.5 scenario; (b) model outputs, mean and maximum-minimum envelopes for the RCP 8.5 scenario; (c) model outputs, means and maximum-minimum envelopes for the RCP4.5 and RCP8.5 scenarios; (d) coefficients of variation of model estimates for the RCP4.5 and RCP8.5 scenarios

Nat. Hazards Earth Syst. Sci. Discuss., https://doi.org/10.5194/nhess-2017-416
Manuscript under review for journal Nat. Hazards Earth Syst. Sci.
Discussion started: 5 December 2017

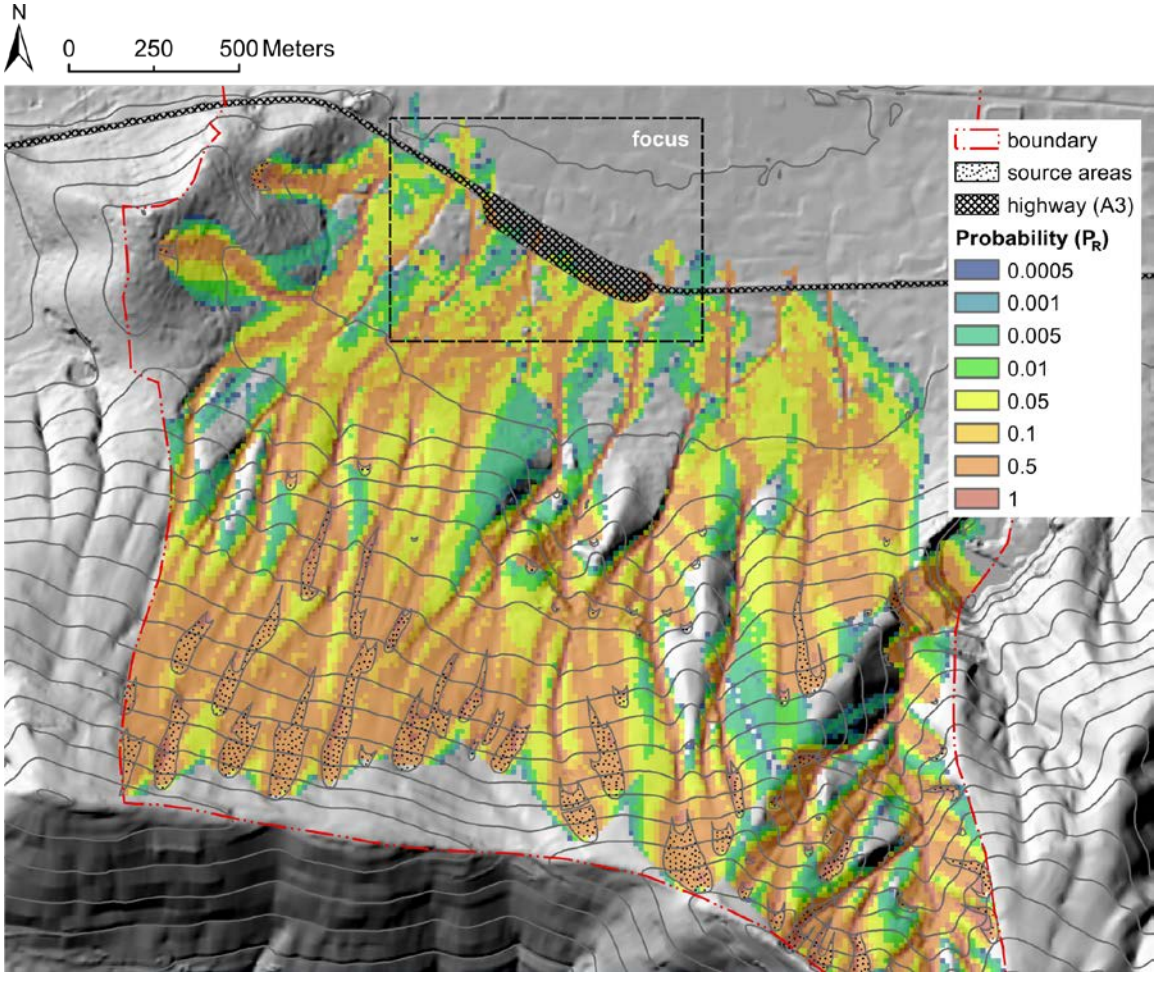

Figure 8. Spatial distribution of reach probability at hillslope scale

Nat. Hazards Earth Syst. Sci. Discuss., https://doi.org/10.5194/nhess-2017-416
Manuscript under review for journal Nat. Hazards Earth Syst. Sci.
Discussion started: 5 December 2017

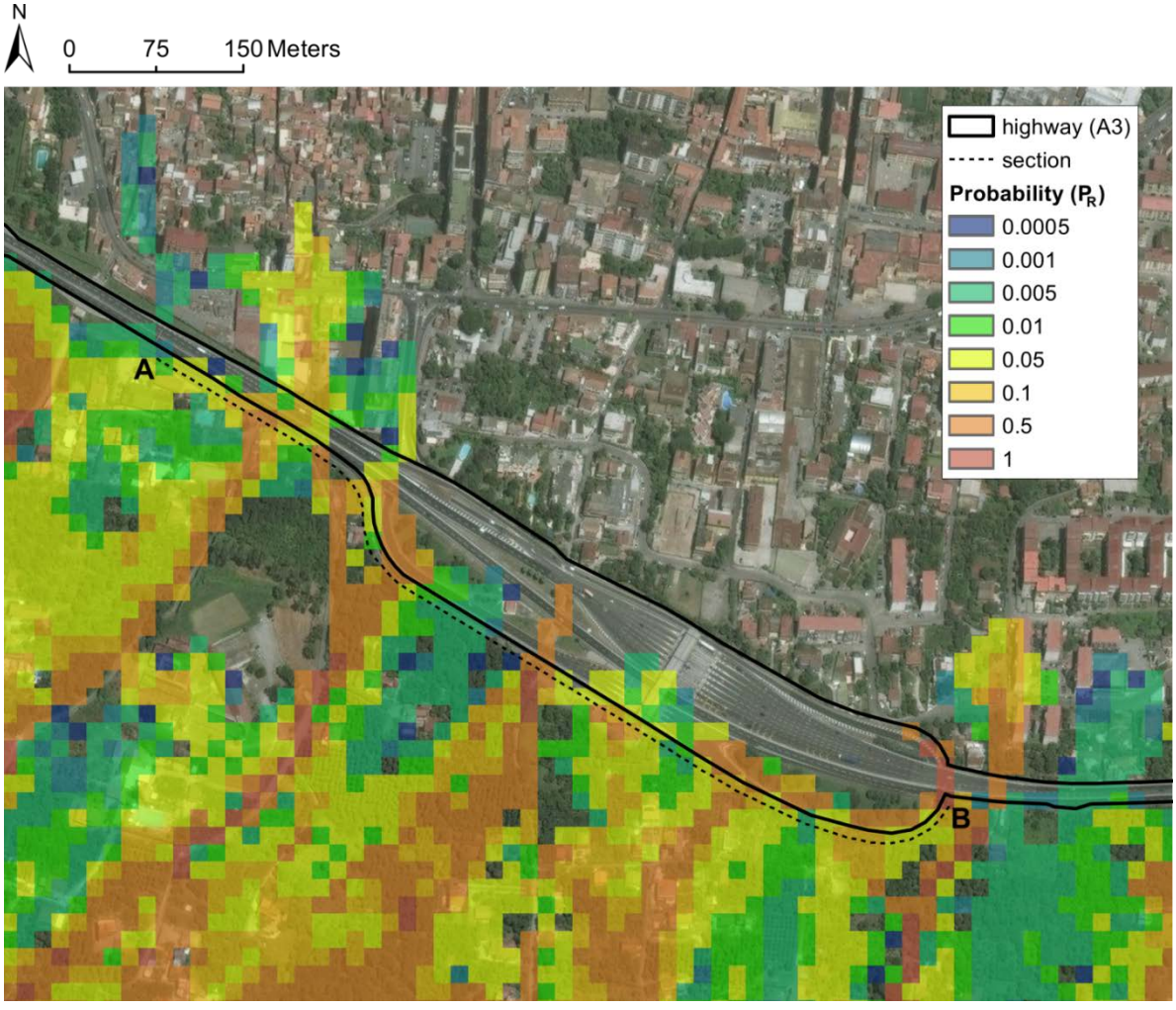

Figure 9. Spatial distribution of reach probability at infrastructure scale

Nat. Hazards Earth Syst. Sci. Discuss., https://doi.org/10.5194/nhess-2017-416
Manuscript under review for journal Nat. Hazards Earth Syst. Sci.
Discussion started: 5 December 2017

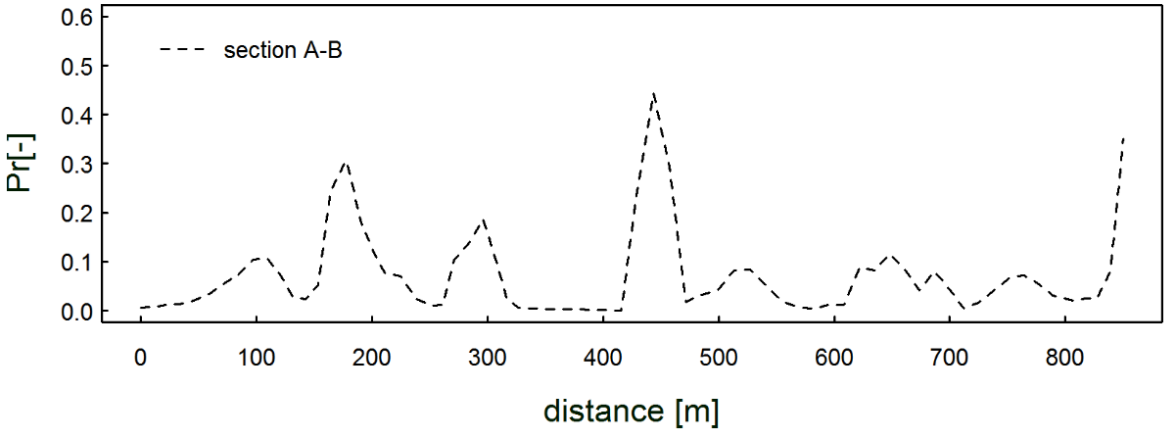

Figure 10. Reach probability along the A-B section of the A3 motorway